Supplemental Figure 1

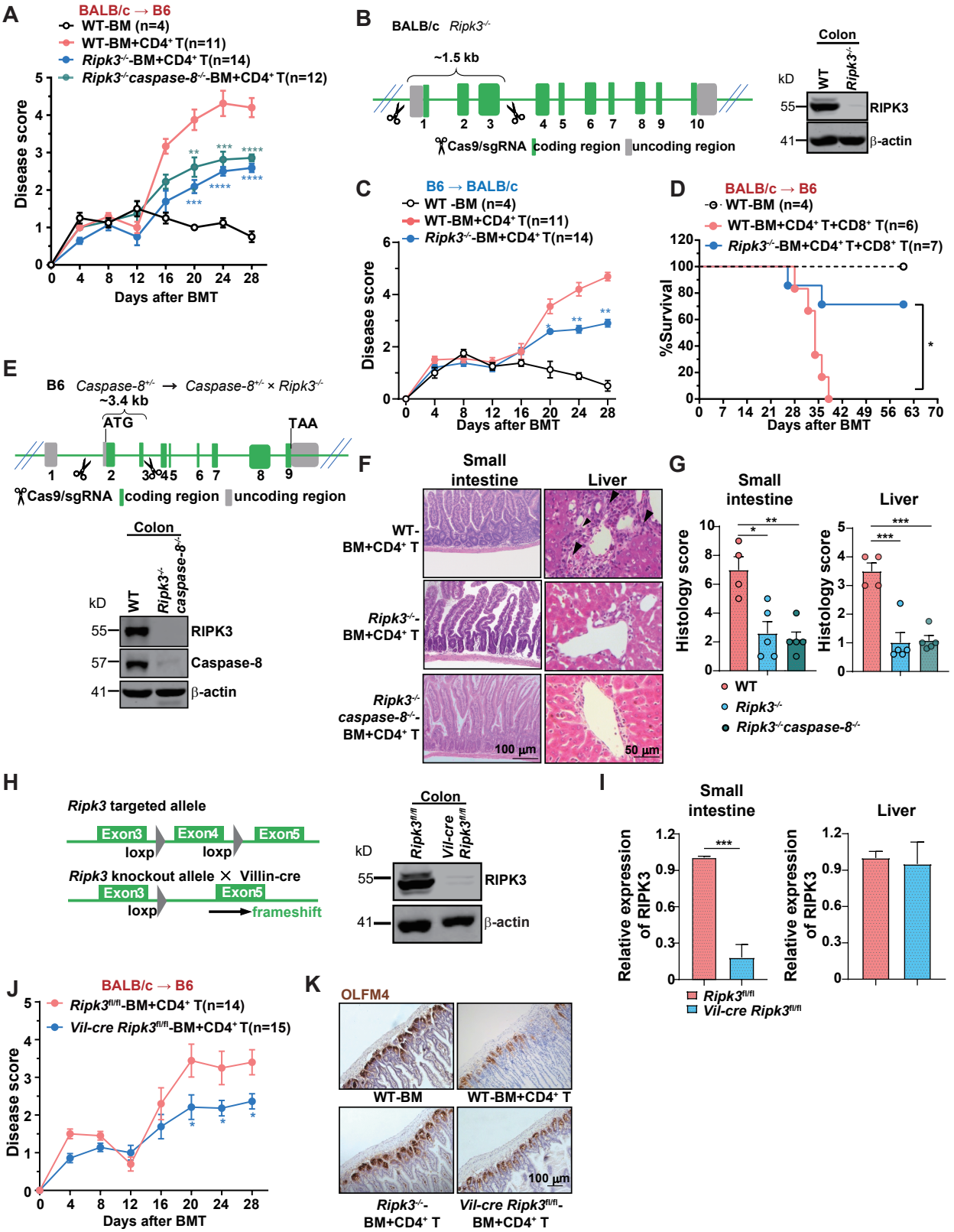

Supplemental Figure 1. Loss of RIPK3 in IECs protects mice from both local and systemic GVHD.
(A) Disease scores were evaluated in the lethally irradiated WT, *Ripk3*$^{-/-}$ and *Ripk3*$^{-/-}$*caspase-8*$^{-/-}$ B6 recipients (BALB/c →B6) that received BALB/c T cell-depleted BM cells (BM) with or without CD4$^+$ T cells (BM+CD4$^+$ T).
(B) Schematic of the strategy for the generation of *Ripk3*$^{-/-}$ BALB/c mice using CRISPR/Cas9 (left). Immunoblotting analysis of RIPK3 and β-actin in the colon from *Ripk3*$^{-/-}$ BALB/c mice and WT littermates (right).
(C) Disease scores were evaluated in the lethally irradiated WT and *Ripk3*$^{-/-}$ BALB/c recipients (B6→BALB/c) that received B6 T cell-depleted BM cells (BM) with or without CD4$^+$ T cells (BM+CD4$^+$ T).
(D) Survival of the lethally irradiated WT and *Ripk3*$^{-/-}$ B6 recipients (BALB/c→B6) that received BALB/c T cell-depleted BM cells (BM) with or without CD4$^+$ T and CD8$^+$ T cells (BM+CD4$^+$ T+ CD8$^+$ T).
(E) *Caspase-8*$^{+/-}$ B6 mice were generated using CRISPR/Cas9 and then crossed with *Ripk3*$^{-/-}$ to generate of *Ripk3*$^{-/-}$*caspase-8*$^{-/-}$ B6 mice (top). Immunoblotting analysis of RIPK3, caspase-8, and β-actin in the colon from WT and *Ripk3*$^{-/-}$*caspase-8*$^{-/-}$ B6 mice (bottom).
(F-G) Histology analysis of small intestine and liver obtained from WT, *Ripk3*$^{-/-}$, and *Ripk3*$^{-/-}$*caspase-8*$^{-/-}$ B6 recipients (BALB/c→B6) on day 17 post allo-HCT. Representative H&E images (F) and quantification of pathology scores (G). Bar in small intestine represents 100 μm. Bar in liver represents 50 μm. Black arrows indicate areas of inflammatory cell infiltration or cell damage.
(H) Schematic of the strategy for generation of *Ripk3*$^{fl/fl}$ B6 mice using CRISPR/Cas9 (left). Immuno-blotting analysis of RIPK3 protein and β-actin levels in the colon of *Vil-cre Ripk3*$^{fl/fl}$ B6 and *Ripk3*$^{fl/fl}$ B6 mice (right).
(I) qPCR analysis of the *Ripk3* mRNA level in the small intestine and liver from *Vil-cre Ripk3*$^{fl/fl}$ and *Ripk3*$^{fl/fl}$ B6 mice.
(J) Disease scores were evaluated in the lethally irradiated *Ripk3*$^{fl/fl}$ and *Vil-cre Ripk3*$^{fl/fl}$ B6 recipients (BALB/c→B6) that received BALB/c T cell-depleted BM cells (BM) with or without CD4$^+$ T cells (BM+CD4$^+$ T).
(K) Representative images of IHC staining of OLFM4 in the small intestine on day 17 post allo-HSC. Bar represents 100 μm.
Data are representative of two or three independent experiments. Data are shown as the mean ± SD (I), others are shown as the mean ± SEM (A, C, G and J). *$p < 0.05$; **$p < 0.01$; ***$p < 0.001$; ****$p < 0.0001$. Disease score comparisons were evaluated by two-way ANOVA (A, C and J). Survival comparisons were evaluated by log-rank test (D). Multiple comparisons were evaluated by one-way ANOVA (G); two-group comparisons used unpaired t tests (two-tailed) (I).

Supplemental Figure 2

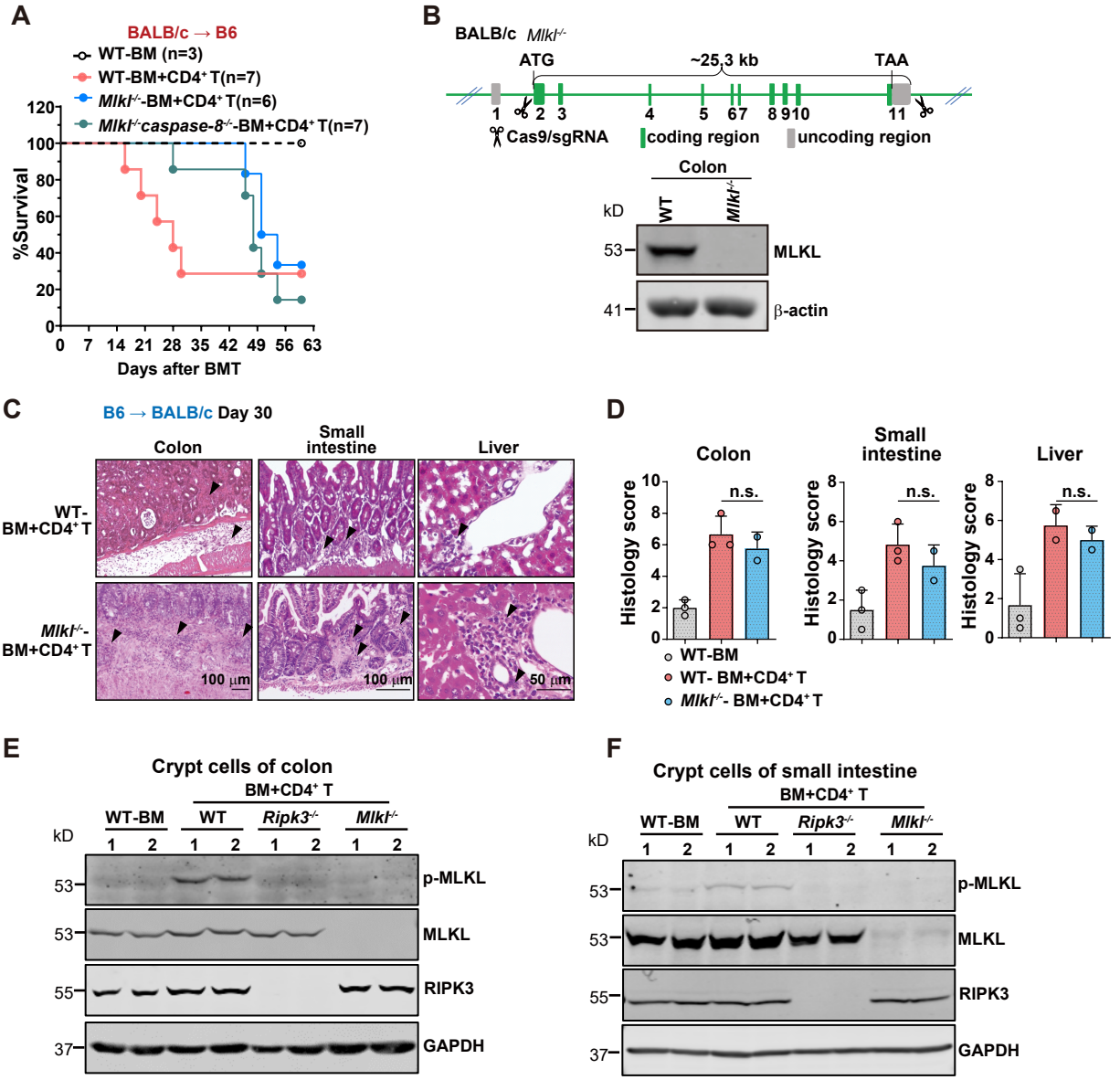

Supplemental Figure 2. RIPK3 promotes necroptosis-independent production of alloreative-T-cell-recruiting chemokines in IECs.

(A) Survival rate of the lethally irradiated WT, *Mlkl*$^{-/-}$, and *Mlkl*$^{-/-}$*caspase-8*$^{-/-}$ B6 recipients (BALB/c→B6) that received BALB/c T cell-depleted BM cells (BM) with or without CD4$^+$ T cells (BM+CD4$^+$ T).

(B) Schematic of the strategy for generation of *Mlkl*$^{-/-}$ BALB/c mice using CRISPR/Cas9 (top). Immunoblotting of MLKL and β-actin in the colon from *Mlkl*$^{-/-}$ BALB/c mice and WT littermates (bottom).

(C-D) The lethally irradiated WT and *Mlkl*$^{-/-}$ BALB/c recipients (B6→BALB/c) received B6 T cell-depleted BM alone (BM) or T cell-depleted BM plus CD4$^+$ T cells (BM+CD4$^+$ T). Histology analysis of colon, small intestine, and liver obtained from the indicated BALB/c mice on day 30 post allo-HCT. Representative H&E images (C) and quantification of pathology scores (D). Bars in colon and small intestine represent 100 μm. Bar in liver represents 50 μm. Black arrows indicate areas of inflammatory cell infiltration or cell damage.

(E-F) Immunoblotting analysis of p-MLKL, MLKL, RIPK3, and GAPDH in the crypt cells of colon(E) and small intestine (F) from the indicated B6 recipients on day 14 post allo-HCT.

Data are representative of three independent experiments. Data are shown as the mean ± SEM; evaluation using one-way ANOVA.

Supplemental Figure 3

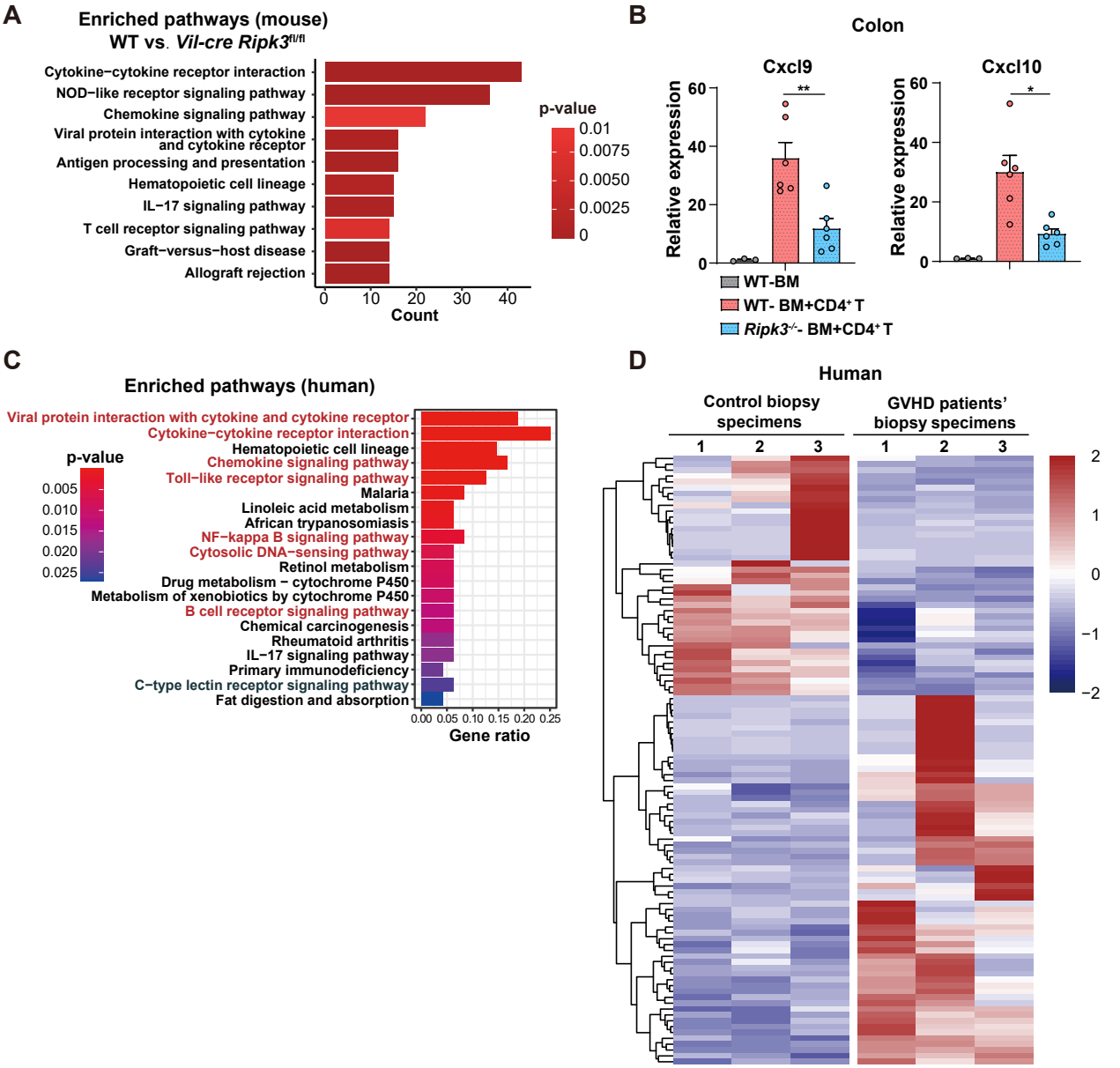

Supplemental Figure 3. RIPK3 promotes necroptosis-independent production of alloreative-T-cell-recruiting chemokines in IECs.

(A) KEGG pathway enrichment analyses of the DEGs in the small intestine collected from WT and *Vil-cre Ripk3*$^{fl/fl}$ mice on day 17 following allo-HCT (p-value<0.05, the p-value is calculated by hypergeometric distribution).

(B) qPCR analysis of *Cxcl9* and *Cxcl10* mRNA levels in the colon from the indicated B6 recipients (BALB/c→B6) 17 days after allo-HCT.

(C) RNA-seq of colonic biopsy specimens from three GVHD patients and three control colonic biopsy specimens from pediatric patients with intractable anal fissure while showing no signs of intestinal injury. Heat map showing 104 Differentially Expressed Genes (DEGs): 63 DEGs were significantly up-regulated and 41 DEGs were significantly down-regulated in the GVHD samples.

(D) KEGG pathway enrichment analyses of the DEGs between control colonic biopsy specimens from non-GVHD children and colonic biopsy specimens from pediatric patients with GVHD (p-value<0.05, the p-value is calculated by hypergeometric distribution).

Data are representative of three independent experiments. Data are shown as the mean ± SD. *p < 0.05; **p < 0.01. Multiple comparisons were evaluated by one-way ANOVA.

Supplemental Figure 4

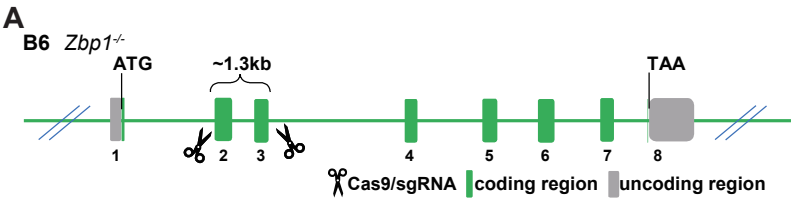

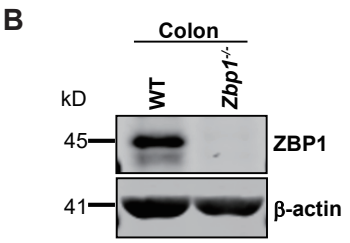

Supplemental Figure 4. Generation of *Zbp1*$^{-/-}$ B6 mice.
(A) Schematic for the generation of *Zbp1*$^{-/-}$ B6 mice using CRISPR/Cas9.
(B) Immunoblotting analysis of ZBP1 and β-actin in the colon from *Zbp1*$^{-/-}$ B6 mice and WT littermates.

Supplemental Figure 5

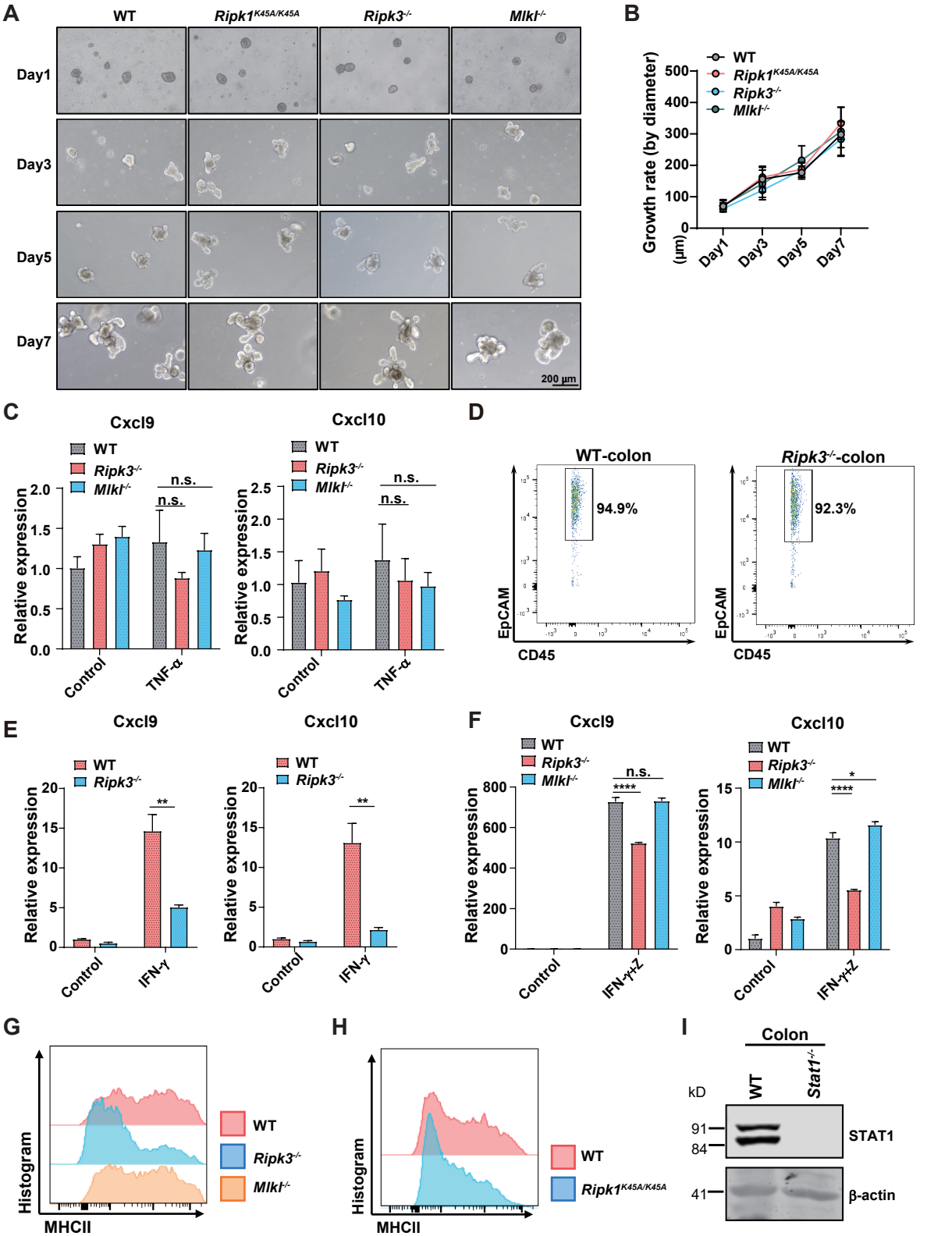

Supplemental Figure 5. IEC RIPK1/RIPK3 engages the JAK/STAT1 signaling to promote expression of chemokines and MHC class II molecules.

(A-B) Representative images (A) and growth rate(B) of small intestinal organoids from B6-WT, *Ripk1*$^{K45A/K45A}$, *Ripk3*$^{-/-}$, and *Mlkl*$^{-/-}$ mice on Day 1, Day 3, Day 5, and Day 7. Bar represents 200 μm.

(C) Small intestinal organoids prepared from WT, *Ripk3*$^{-/-}$, and *Mlkl*$^{-/-}$ B6 mice were treated with control or TNF-α (100 ng/ml) for 12h, with qPCR measurement of *Cxcl9* and *Cxcl10* expression.

(D) The percentage of isolated IEC in the colon was analyzed. Representative flow plots are shown.

(E) Purified IEC from WT and *Ripk3*$^{-/-}$ B6 mice were treated with control (PBS) or IFN-γ (10 ng/ml) for 12h, with qPCR measurement of *Cxcl9* and *Cxcl10* expression.

(F) Small intestinal organoids prepared from WT, *Ripk3*$^{-/-}$, and *Mlkl*$^{-/-}$ B6 mice were treated with the pan-caspase inhibitor z-VAD (20 μM) for 2h prior to IFN-γ treatment for 12 h. qPCR measurement of *Cxcl9* and *Cxcl10* expression.

(G-H) MHC class II expression in the small intestinal organoids was analyzed. The organoids prepared from WT, *Ripk3*$^{-/-}$, and *Mlkl*$^{-/-}$ B6 mice (G) or WT, *Ripk1*$^{K45A/K45A}$ B6 mice (H) were treated with control (PBS) or IFN-γ (10 ng/ml) for 24h. Representative flow plots are shown.

(I) Immunoblotting analysis of STAT1 and β-actin in the colon from WT and *Stat1*$^{-/-}$ B6 mice.

Data are representative of three independent experiments. Data are shown as the mean ± SD. *p < 0.05; **p < 0.01; ****p < 0.0001. Multiple comparisons were evaluated by one-way ANOVA (C, F), two-group comparisons by unpaired t tests (two-tailed) (E).

Supplemental Figure 6

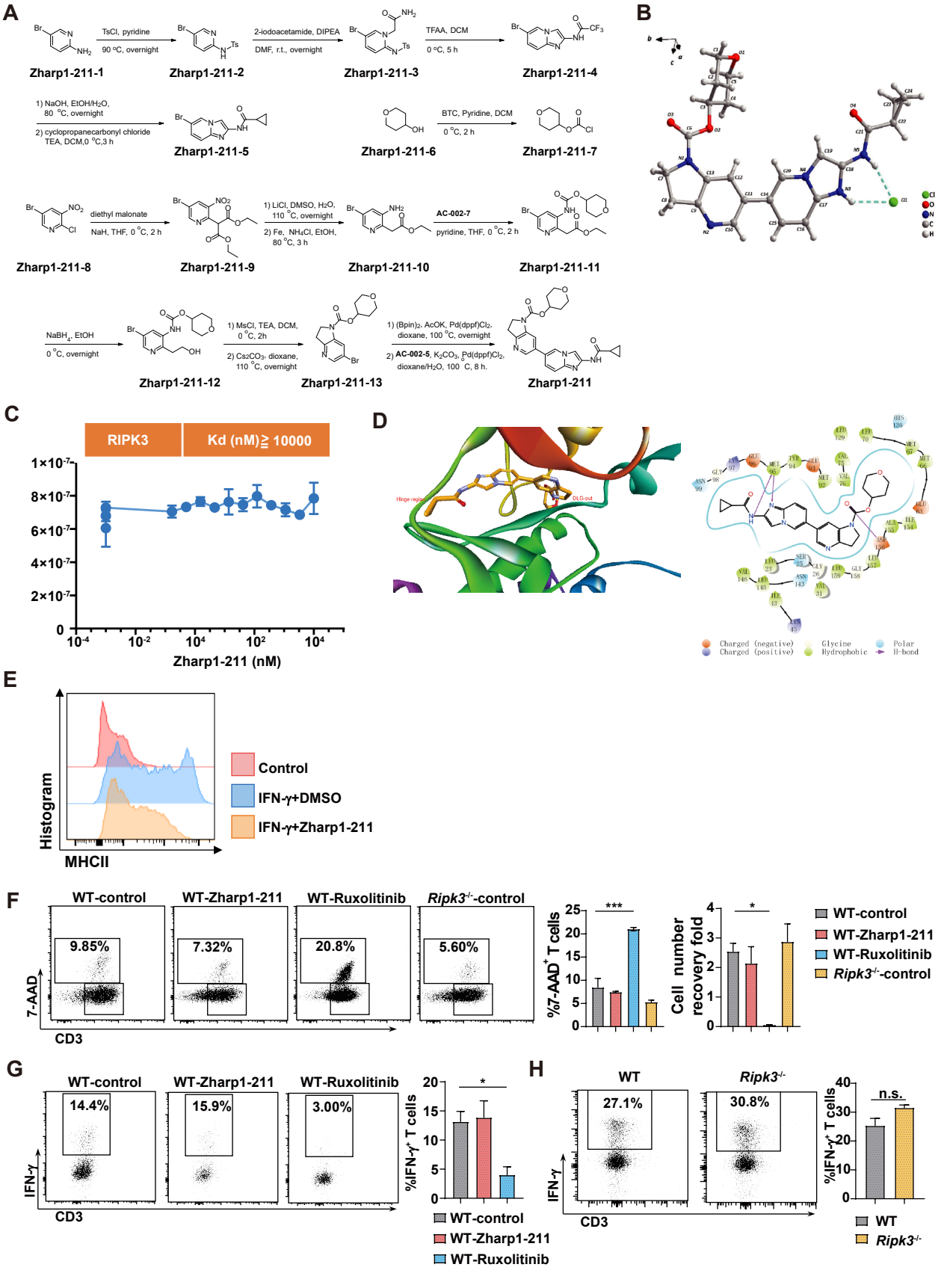

Supplemental Figure 6. Development of a novel RIPK1 kinase inhibitor reducing JAK/STAT1-mediated expression of chemokines and MHC class II molecules in IECs.

(A) The synthesis route for Zharp1-211.

(B) The crystal structure of Zharp1-211 with one molecule of HCl.

(C) The binding constant (Kd) of Zharp1-211 with human recombinant RIPK3.

(D) A molecular docking study, suggesting that Zharp1-211 functions as a type II inhibitor of RIPK1. The docking indicated that the N-acetamide group of Zharp1-211 forms a hydrogen bond with the backbone CO of RIPK1's residue Met95 in the hinge region, and that the carbonyl oxygen of the carbamic acid group forms a hydrogen bond interaction with the backbone amide of residue Asp156 of the DLG motif. Additionally, the CO of residue Met95 also has a tight interaction with the imidazo[1,2-a]pyridine group of Zharp1-211 (hydrogen bond interaction). In the head group of Zharp1-211, the tetrahydro-2H-pyran group is buried deeply in the allosteric hydrophobic back pocket comprising residues Met66, Met67, and Leu70.

(E) MHC class II expression in the small intestinal organoids was analyzed. The organoids prepared from B6 mice were pretreated with Zharp1-211 (100 nM) for 2h prior to the treatment with IFN-γ (10 ng/ml) for 24h. Representative flow plots are shown.

(F-H) $CD3^+$ T cells were purified from the indicated B6 mice, labeled with CellTrace violet, and stimulated with CD3 and CD28 antibodies. $CD3^+$ T cells were treated with control (DMSO) or 100 nM Zharp1-211 or 300 nM ruxolitinib. Five days later, T cells were collected to measure their survival rate and proliferation (F). Dot plots and graphs show the percentages of IFN-γ producing cells among $CD3^+$ T cells (G-H).

Data are representative of three independent experiments. Data are shown as the mean ± SD. *$p < 0.05$; ***$p < 0.001$. Multiple comparisons were evaluated by one-way ANOVA (F-G), two-group comparisons by unpaired t tests (two-tailed) (H).

Supplemental Figure 7

Zharp1-211	
Physicochemical properties	
M.W.	448
cLogP[a]	2.9
Pka[b]	6.0
PSA[a]	98
Solubility[c] (μg/mL)	2.3
Caco-2 (A to B(10^{-6} cm/s)/ Ratio)	15/4.2
Disposition and Safety profiles	
PPB Bound % (human, rat, mouse)	93.4/95.5/96.1
CYP inhibition@ 10 μM (3A4, 1A2, 2D6, 2C9 and 2C19)	-21/3/3/33/36
hERG IC_{50} (μM)	>30

[a] Calculated by Molinspiration.

[b] Calculated by ACD/Labs 6.0.

[c] Data was measured duplicates in pH= 6.5 FaSSIF using LC-MS/MS.

Supplemental Figure 7. Physicochemical properties and in vitro safety profile of Zharp1-211.
Zharp1-211 (HCl salt) were evaluated for its inhibitory potency against human P450 enzymes in human liver microsomes and for block of the hERG potassium channel at Chempartner using CHO cells stably expressing the hERG gene and the QPatch platform (Sophion, Ballerup, Denmark).

Supplemental Figure 8

Species	Mice		Rat	
Dose	IV (2 mg/kg)	PO (10 mg/kg)	IV (2 mg/kg)	PO (10 mg/kg)
T_{max} (h)	0.08	0.5	0.08	1.0
Cmax (ng/mL)	1411	1963	1396	1328
AUC_{0-24} (ng/mL*h)	456	2875	1100	3690
$t_{1/2}$ (h)	0.8	1.0	1.2	1.5
CL (mL/min/kg)	71		31	
$V_{d, ss}$ (L/kg)	4.8		3.1	
F (%)		126		67

Supplemental Figure 8. Pharmacokinetics of Zharp1-211.
Plasma pharmacokinetic parameters of per oral (PO) and intravenous injection (IV) in mice and rat.

Supplemental Figure 9

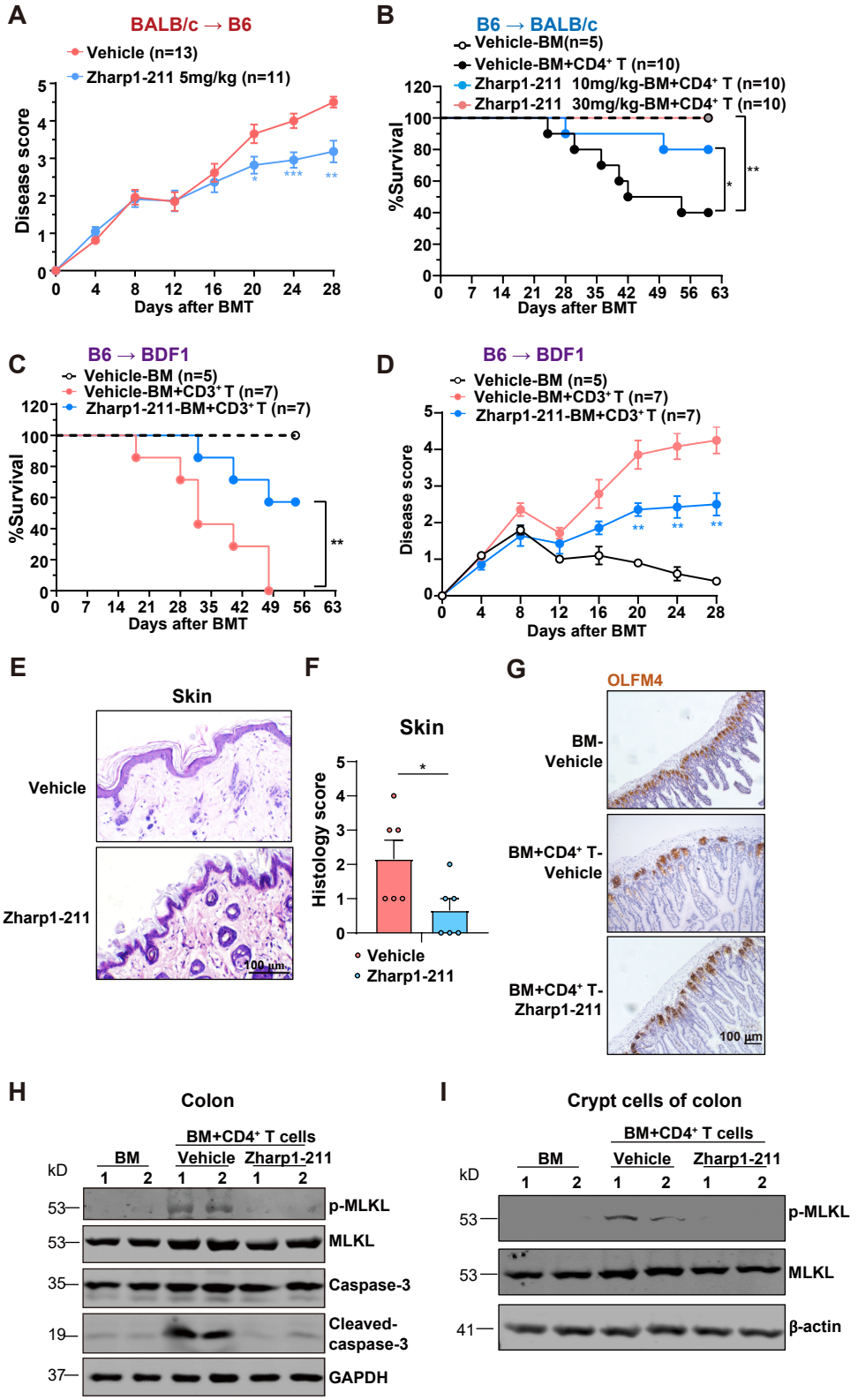

Supplemental Figure 9. Pharmacological inhibition of RIPK1 reduces ongoing GVHD.
(A, E-G) The lethally irradiated B6 recipients (BALB/c→B6) received BALB/c T cell-depleted BM cells with $CD4^+$ T cells. Starting at 7 days post allo-HCT, mice were treated daily (intraperitoneally) with vehicle or Zharp1-211 (5mg/kg). (A) Disease scores of mice post allo-HCT.
(B) The lethally irradiated BALB/c recipients received T cell-depleted BM cells (BM) alone, or in combination with 4×10^5 $CD4^+$ T cells from B6 mice. Starting at 7 days post allo-HCT, recipients were treated with vehicle or Zharp1-211 by oral gavage (10mg/kg or 30mg/kg, twice daily). Survival curves were analyzed.
(C-D) The lethally irradiated BDF1 recipients (B6→BDF1) received B6 T cell-depleted BM cells with $CD3^+$ T cells. Starting at 7 days post allo-HCT, mice were treated daily (intraperitoneally) with vehicle or Zharp1-211 (5mg/kg). Survival (C) and disease scores (D) of mice post allo-HCT.
(E-F) Histological analysis of skin, assessed on day 17 post allo-HCT. Representative H&E images (E) and quantification of pathology scores (F). Bar represents 100 μm.
(G) Representative images of IHC staining of OLFM4 in small intestines on day 17 post allo-HSC. Bar represents 100 μm.
(H-I) Immunoblotting analysis of p-MLKL, MLKL, caspase-3, cleaved caspase-3, and GAPDH in the colon or crypt cells of colon from the indicated B6 recipients on day 14 post allo-HCT.
Data are representative of two independent experiments. Data are shown as the mean ± SEM. *$p < 0.05$; **$p < 0.01$. Survival comparisons were evaluated by log-rank test (B-C). Disease score comparisons were evaluated by two-way ANOVA (A, D). Two-group comparisons by unpaired t tests (two-tailed) (F).

Supplemental Figure 10

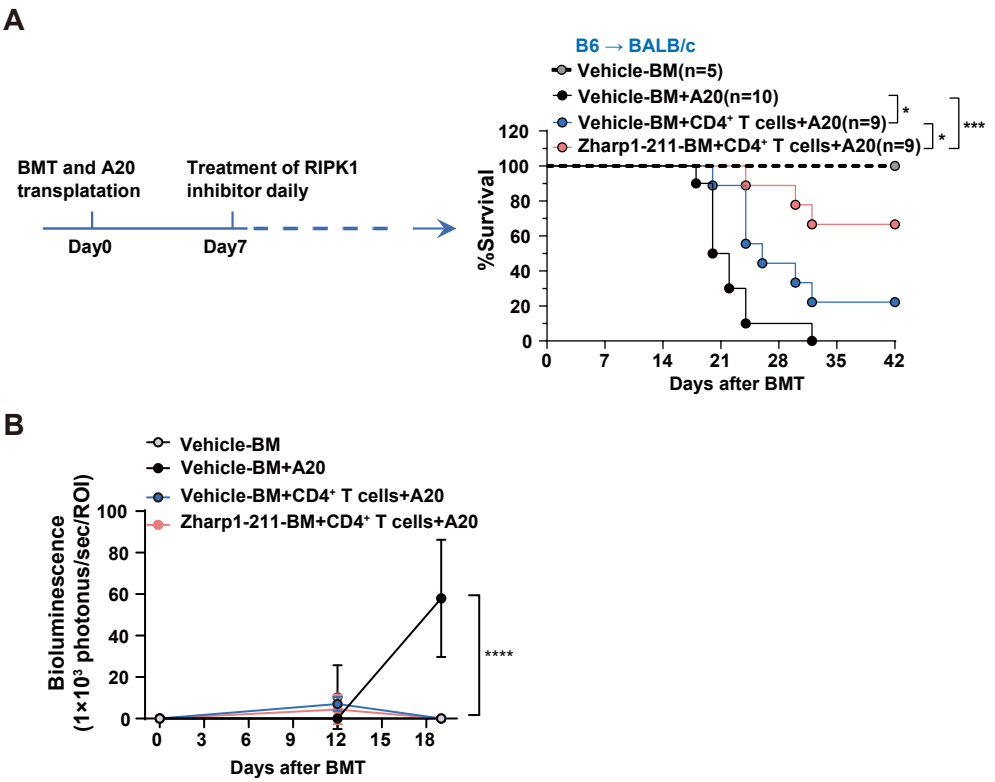

Supplemental Figure 10. Pharmacological inhibition of RIPK1 reduces ongoing GVHD without compromising the GVL effect.

(A-B) The lethally irradiated BALB/c recipients received T cell-depleted BM cells (BM) alone, or in combination with $CD4^+$ T cells from B6 mice. Subsequently, these mice were challenged with 1×10^6 A20 lymphoma cells at the time of the BM transplant. Starting at 7 days post allo-HCT, recipients were treated daily (intraperitoneally) with vehicle or Zharp1-211 (5mg/kg). The survival rates (A) and bioluminescence measurements (B) were shown.

Data are representative of two independent experiments. Data are shown as the mean ± SEM. *$p < 0.05$; ***$p < 0.001$; ****$p < 0.0001$. Survival comparisons were evaluated by log-rank test (A). Bioluminescence measurements comparisons were evaluated by two-way ANOVA (B).

Supplemental Figure 11

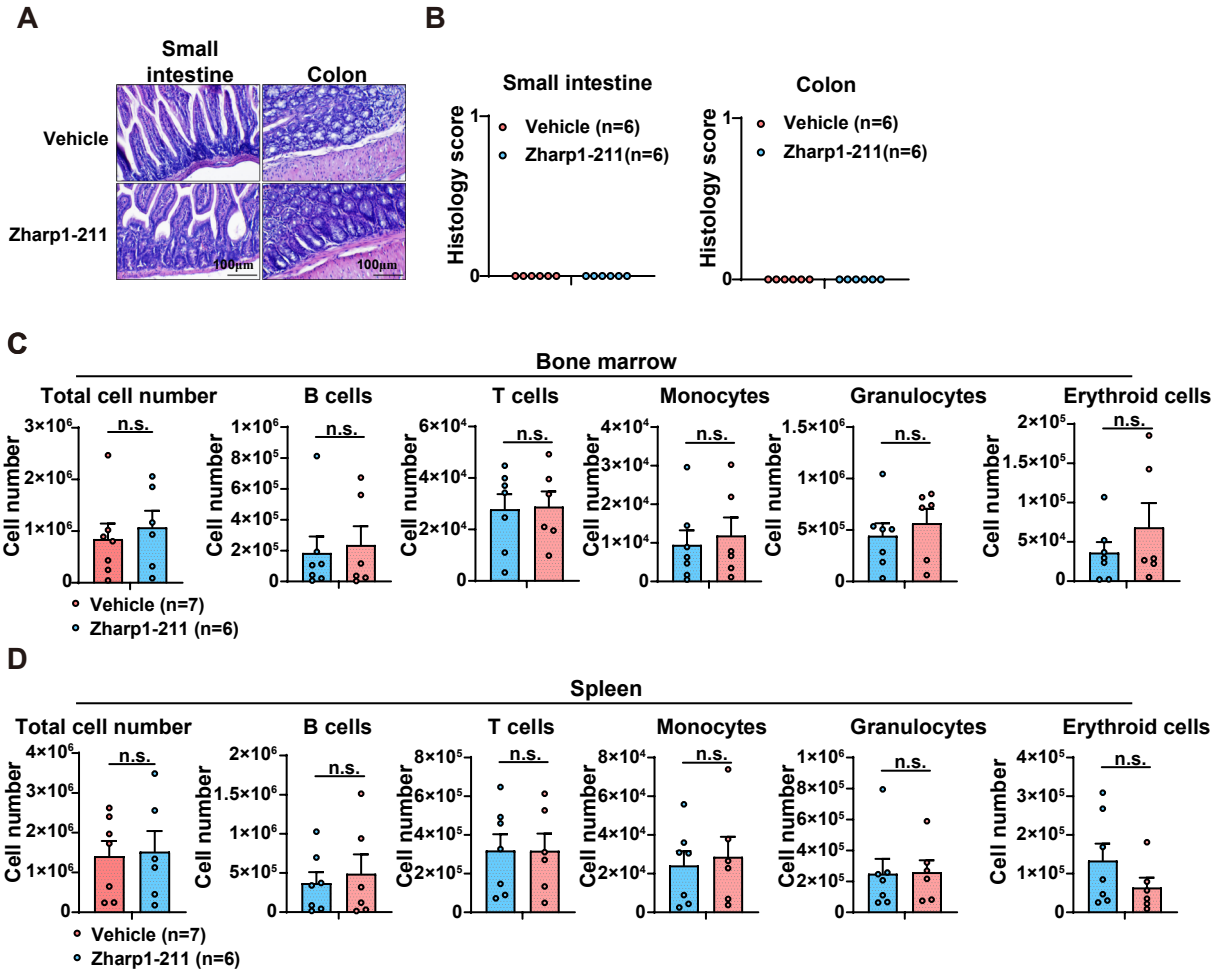

Supplemental Figure 11. Effect of Zharp1-211 on IECs and bone marrow reconstruction.
(A-B) BALB/c mice were treated daily (intraperitoneally) with vehicle or Zharp1-211 (5mg/kg) for 2 weeks. Representative H&E images (A) and quantification of pathology scores (B).
(C-D) Lethally irradiated B6 recipients (B6→BALB/c) received B6 T cell-depleted BM cells. Starting at 7 days post allo-HCT, mice were treated daily (intraperitoneally) with vehicle or Zharp1-211 (5mg/kg). Total cell numbers and percentage of T cells, B cells, granulocytes, monocytes, erythroid cells were evaluated in bone marrow (C) and spleen (D).
Data are representative of two independent experiments. Data are shown as the mean ± SEM. Two-group comparisons by unpaired t tests (two-tailed).

Supplementary Materials and methods

Mice models of GVHD

Male mice at 8 to 10 weeks of age were used as recipients. BM transplantation recipient mice were fed with antibiotics in drinking water containing 0.5 mg/ml neomycin (97061-908, VWR) and 12.8 μg/ml polymyxin B (P1004, Sigma) for 3 days. The B6 recipient mice were total body irradiated with 9.5 Gy (split doses of 2 × 4.75 Gy apart to 4 h). The BALB/c recipient mice were total body irradiated with 6.5 Gy (split doses of 2 × 3.25 Gy apart to 4 h). The BDF1 recipient mice were total body irradiated with 9.5 Gy (split doses of 2 × 4.75 Gy apart to 4 h). Donor BM cells were depleted of T cells using CD4 positive purification beads (130-117-043, Miltenyi) and CD8 positive purification beads (130-117-044, Miltenyi). Donor T cells were isolated using the enrichment CD8 microbeads, CD4 microbeads, and CD3 microbeads (480024, Biolegend). Donor T cell-depleted BM and CD4 T, CD8 T or CD3 T cells were then used for transplantation as follows: B6 →BALB/c (1×10^7 B6 TCD-BM cells with or without 5×10^5 CD4 T cells) and BALB/c → B6 (1×10^7 BALB/c TCD-BM cells with or without 1.5×10^6 CD4 T cells or 5×10^5 CD4 T cells plus 5×10^5 CD8 T cells). B6 →BDF1 (1×10^7 B6 TCD-BM cells with or without 2.5×10^6 CD3 T cells). For GVL experiments using A20 cells, BALB/c recipient mice were intravenously injected with 1×10^6 A20 cells at the time of BM transplant. For GVL experiments using APL cells, B6 recipient mice were intravenously injected with 1×10^6 APL cells at the time BM transplant. In both GVHD and GVL experiments, recipient mice were monitored every 2 days for survival and disease score according to 6 clinical parameters (weight loss, hunched posture, activity, diarrhea, fur texture, and skin lesions) on a scale from 0 to 2 as previously described [1].

Cell lines

The cell line HT-29 is a human colon epithelial cell line, obtained from the American Type Culture Collection (HTB-38, ATCC). The cell line L929 (CCL-1, ATCC) is a mouse fibroblast cell line and was used to study the necroptosis signaling. The cell line A20 (TIB-208, ATCC) is a B cell lymphoma cell line and was infected with luciferase

expressing lentivirus (Genechem) to stably express the luciferase gene. Luciferase expressing A20 cell line was used for bioluminescence assays in the GVL model. The mouse myeloid-related protein 8-promyelocytic leukemia/retinoic acid receptor-a(hMRP8-PML/RAR-a)–harboring acute promyelocytic leukemia (APL) cells were kindly provided by Dr. Jiang Zhu (Institute of Hematology, National Research Center for Translational Medicine, Shanghai). HT-29 and L929 cells were cultured in DMEM supplemented with 10% FBS, glutamine, and antibiotics. A20 cells were maintained in RPMI-1640 medium supplemented with 10% FBS, glutamine, and antibiotics. All cells were maintained at 37°C and 5% CO_2.

Reagents

Mouse TNF-α recombinant protein (Z02774) was purchased from Genscript. The Smac mimetic compound was kindly provided by Dr. Xiaodong Wang (National Institute of Biological Sciences, Beijing). z-VAD (4026865) was purchased from Bachem. Ruxolitinib (S1378) was purchased from Selleck. D-luciferin (115144-35-9) was purchased from Goldbio.

Cell viability assay

Cells were seeded in 96-well plates and then treated as indicated. The cell viability was determined by ATP levels using a CellTiter-Glo Luminescent Cell Viability Assay kit (G7570, Promega) following the manufacturer's instructions. Luminescence was measured with SpectraMax i3x (Molecular Devices).

Western blot analysis and immunoprecipitation

Protein samples were extracted from cell pellets or tissues after harvest. Cell pellets were re-suspended in lysis buffer (20 mM Tris-HCl, pH 7.4, 150 mM NaCl, 10% glycerol, 1% Triton X-100, 1 mM Na_3VO_4, 25 mM β-glycerol-phosphate, 0.1mM PMSF, Roche complete protease inhibitor set and Sigma phosphatase inhibitor set). The mouse tissues or human intestinal explants were ground and re-suspended in lysis buffer plus 0.1% SDS. Samples were vortexed for 20 seconds and then incubated on ice for 20 min. After centrifugation at 20,000 g for 30 min, the supernatants were

collected for western-blot (immunoblotting) analysis. The following antibodies were used for western-blot: RIPK1 (610458, BD bioscience), Mouse RIPK3 (2283, Prosci, CA, USA), GAPDH (3783, Prosci), Mouse MLKL (AP14272b, Abgent, CA, USA), Mouse p-MLKL (ab196436, Abcam, UK), ZBP1 (sc-67258; Santa Cruz, TX, USA), β-actin (A2066, Sigma-aldrich, MO, USA), Mouse p-RIPK1 (BX60008, Biolynx, China), Human p-RIPK1 (65746, CST, MA, USA), caspase-8 (9746, CST), JAK1 (3344, CST), STAT1 (14994, CST), p-STAT1-Y701 (9167, CST), caspase-3 (9662, CST), cleaved caspase-3 (9661, CST), Flag-tag (A8592, Sigma-aldrich), HA-tag (3724, CST), c-Myc-tag (16286-1-AP, Proteintech), anti-Mouse IgG Secondary Antibody (92632210, Li-COR biosciences, NE, USA) and anti-Rabbit IgG Secondary Antibody (92632211, Li-COR biosciences, NE, USA). For Flag immunoprecipitation, cell lysates were incubated with anti-Flag M2 agarose beads (A2220, Sigma, MO, USA) at 4ºC for 12-16h. Agarose beads were washed six times with lysis buffer, and the immunoprecipitants were eluted by incubating them with IgG elution buffer (21004, Thermo, USA).

Measurement of cytokines

The levels of TNF-α and IFN-γ in serum were analyzed using a Cytometric Bead Array (CBA) Mouse Inflammation Kit (552364, BD) according to the manufacturer's instructions.

Drug treatment *in vivo*

Zharp1-211 was diluted into sterile PBS containing 40% PEG400. The B6 or BALB/c recipient mice were administered with vehicle or Zharp1-211 by intraperitoneal injection (5mg/kg, daily) or by oral gavage (10~30mg/kg, twice daily) from the 7th day after BM transplantation.

Histology and immunohistochemistry

The small intestine, colon, and liver samples were collected and fixed with paraformaldehyde (4%). Tissue samples were then embedded in paraffin wax and sections of 4 mm thickness were used for hematoxylin and eosin (H&E) or immunohistochemistry (IHC) staining, followed by the analysis using Nikon Eclipse Ti

with DS-Fi2 camera. Images were processed and quantified using ImageJ.

Histopathological scores were assessed on these H&E stained sections according to acute GVHD grading system as previously described [2,3].

IHC for human p-RIPK1 (65746, CST) and OLFM4 (39141, CST) staining was performed using the Immunohistochemistry Application solution Kit (13079S, CST), according to the manufacturer's instructions. Appropriate positive and negative controls were run in parallel. For phospho-RIPK1 signal analysis, six fields (400 × magnification) with positive signals were randomly selected for each sample. The percentage of phospho-RIPK1-positive glands were quantified.

Immunofluorescence confocal microscopy

Small intestine was collected, paraformaldehyde (4%) fixed, embedded in paraffin, and sectioned. For immunofluorescence confocal microscopy, the section of small intestine was performed using a TSA Signal Amplification kit (NEL701A001KT, PerkinElmer) according to the manufacturer's instructions. Briefly, sections were deparaffinized and underwent antigen retrieval in sodium citrate buffer (pH 6.0) in a heater for 15 min and blocked with 10% goat serum solution followed by a primary antibody incubation overnight at 4 °C. Sections were incubated with an HRP conjugated goat-anti-rabbit secondary antibody and fluorescence-conjugated TSA substrate. Afterward, sections were stained with DAPI (C1002, Beyotime) to label the nuclei. Confocal images were taken using Leica TCS SP8 MP. 3-D confocal images were performed with Leica Application Suite X software. Numbers of $CD3^+$ T cells were counted in representative images of small intestine tissues. The experiment was performed on n>3 mice individually and five visual fields were counted for each sample. Lysozyme (A0099) was purchased from Dako. OLFM4 and CD3 (78588) were purchased from CST.

Culture of murine and human intestinal organoids

Small intestinal crypts were isolated according to the manufacturer's instructions (06005, STEMCELL Technologies). Briefly, small intestines from mice were harvested and rinsed ~ 20 times with PBS prior to incubation with 5mM EDTA in PBS for 15min. Cells were collected after 70 μm filter, resuspended in 40 μl Matrigel Matrix (354234,

Corning) and seeded in 24-well plates. After incubation at 37°C for 15min, IntestiCult Organoid Growth Medium was added into wells. The culture medium was changed every 3 days. After 4 days, the mouse intestinal organoids were used for further analysis.

To generate human colonic organoids, the para-carcinoma tissues from colorectal cancer patients were cut into the smallest pieces possible and incubated in cold PBS containing 10 mM EDTA for 30min on ice with shaking. Then the supernatant was aspirated to isolate crypts and filtered through a 70-μm strainer and centrifuged at 250 g for 5 min to gather crypts. Crypts were resuspended in 40 μl Matrigel Matrix and seeded in 24-well plates. After incubation at 37°C for 15min, IntestiCult Organoid Growth Medium (06010, STEMCELL Technologies) was added into wells. The culture medium was changed every 2 days. After 4 days culture, the human colonic organoids were used for further analysis. Organoids were imaged using a Nikon Eclipse Ti2 and Oplenic camera. For organoid viability assays, crypts were embedded in 10 μl Matrigel at 5,000 crypts/ml and seeded in a 96-well culture plate. After 24h, organoids were stimulated as indicated for further analysis. Cell viability was determined by using a CellTiter-Glo Luminescent Cell Viability Assay kit (Promega). For chemokine detection organoids were embedded in 20 μl Matrigel at 5,000 crypts/ml and seeded in a 48-well culture plate. After 24h, organoids were stimulated as indicated for further analysis. The expression of chemokines was determined by qPCR or Elisa analysis.

Proximity ligation assay

Intestinal crypt cells were isolated from WT B6 mice and treated with IFN-γ for 4h. Cells were collected and fixed with paraformaldehyde (4%), permeabilized with 0.2% TritonX-100 for 10 min, and blocked in Blocking buffer for 1 h. After incubation with primary antibodies (mouse anti-RIPK1 antibody: 1:50 and rabbit anti-JAK1: 1:50 in antibody dilution buffer overnight at 4℃. Then cells were subjected to PLA (Duolink In Situ Detection Reagents Red, DUO92008, Sigma) with anti-mouse (Duolink In Situ PLA Probe Anti-Mouse MINUS, DUO92001, Sigma) and anti-rabbit (Duolink In Situ PLA Probe Anti-Rabbit PLUS, DUO92005, SIGMA) secondary antibodies, according to the manufacturer guidelines. Afterward, cells were stained with DAPI (C1002, Beyotime) to label the nuclei. Confocal images were taken using Leica TCS SP8 MP.

Chromatin immunoprecipitation (ChIP) assays

Following the 0.5h treatments with IFN-γ, approximately 1×10^8 intestinal crypt cells were cross-linked for 10 min by the addition of 0.75% formaldehyde. Cross-linking was stopped by the addition of glycine to a final concentration of 125 mM for 5 min. The cells were collected and washed once with ice cold phosphate buffered saline. Cell pellets were lysed in 200μl ChIP Lysis Buffer (50 mM Hepes-KOH at pH 7.5; 1 mM EDTA; 140 mM NaCl; 0.1% Sodium Deoxycholate; 0.1% SDS; 1% Triton X-100; 1 × protease inhibitor cocktail) and incubated for 10 min at 4°C. Samples were sonicated with Covaris S220 with a microtip in 20s bursts followed by 30s of cooling for a total sonication time of 1 min per sample. This procedure resulted in DNA fragment sizes of about 300-1000bp. Each sample was diluted 1:10 with RIPA Buffer (50 mM Tris-HCl pH8; 150 mM NaCl; 2 mM EDTA pH8; 1% NP-40; 0.5% Sodium Deoxycholate; 0.1% SDS; 1×Protease Inhibitors). Samples were then centrifuged at 8,000g for 10 min at 4°C. Either 5 μg of STAT1 antibody or 5 μg of IgG antibody were added to 500 μl aliquots of extract and incubated at 4°C overnight. Samples were transferred to tubes containing 30 μl of prewashed Protein A beads. After 2 h incubation, samples were centrifuged at 6000 rpm and the beads were washed three times: once in low salt wash buffer (0.1% SDS; 1% Triton X-100; 2 mM EDTA; 20 mM Tris-HCl pH 8.0; 150 mM NaCl), once in high salt wash buffer (0.1% SDS; 1% Triton X-100; 2 mM EDTA; 20 mM Tris-HCl pH 8.0; 500 mM NaCl), once in LiCl wash buffer (0.25 M LiCl; 1% NP-40; 1% Sodium Deoxycholate 1 mM EDTA; 10 mM Tris-HCl pH 8.0). Then, 120 μl of Elution buffer was added (1% SDS; 100mM $NaHCO_3$) and vortex slowly for 15 min at 30°C. The supernatant was transferred into a fresh tube adding 4.8 μL of 5 M NaCl and 2 μL RNase A (10 mg/mL with incubation at 65°C overnight. Then, 2 μL proteinase K (20 mg/mL) was added and incubated while shaking at 60°C for 1 h. DNA was purified through phenol-Chloroform-Isoamyl Alcohol extraction. The PCR reaction was performed on the Roche LightCycler 480 II system with primers following:

Cxcl9-F: 5′- AGCTTTGACTTGTGAGGAAAGG -3′

Cxcl9-R: 5′- TATTGAGTCACTGTGTTGGAGTTGA -3′

Cxcl10-F: 5′- GCCTCTGCTTCTGAGCTTCTTCTAAG -3′

Cxcl10-R: 5′- GGCACATTTGCTTCGCTAGTATTTATTC -3′

T cell analysis

$CD3^+$ T cells were purified with CD3 microbeads (480024, Biolegend,) and labeled with CellTrace violet (C34571, Invitrogen,) following the manufacturer's instructions. 5×10^7 T cells were seeded in a 96 well plate coated with anti-CD3 antibody (100223, Biolegend). T cells were maintained with anti-CD28 antibody (102116, Biolegend) and 50 U/ml of IL2 (212-12, PeproTech) from day 1. All measurements of cell composition and number were performed in duplicate. All samples were examined with an Attune NxT Flow Cytometer (Invitrogen), and data analyses were performed using FlowJo (BD Biosciences).

Intestinal crypt cells isolation

Intestinal crypts from mice were isolated as previously described[4], with slight modifications. Briefly, intestines were prepared by cut into two cm^2 pieces in ice-cold PBS and digested in Gentle Cell Dissociation Reagent (100-0485, STEMCELL) with shaking (20 rpm) for 15min, then carefully removed the supernatant and washed twice in PBS. The remaining tissue was resuspended in PBS and pipetted up and down. The supernatant was centrifuged to gather crypts. The crypts were seeded into dishes pre-coated with 1 μg/ml type I collagen for 30 min. The dishes were washed with PBS twice to remove immune cells. The remaining cells were collected for the indicated stimuli.

Treatment of human intestinal explants

Human surgical intestinal explants were isolated as previously described [5]. Briefly, intestinal specimens were cut into small pieces (around 3 mm^3) and then cultured in RPMI 1640 medium containing 10% fetal bovine serum and antibiotics at 37℃ and 5% CO_2. Human intestinal explants were treated with RIPK1 kinase inhibitor Zharp1-211

or ruxolitinib for 2h prior to IFN-γ (315-05, Peprotech) treatment, and then were collected for further western blot analysis.

Molecular docking study

For investigating the interaction mechanism between Zharp1-211 and RIPK1, Zharp1-211 was docked into the binding site of the RIPK1 crystal complex (PDB ID: 4NEU) [6] from RCSB Protein Data Bank by employing the extra precision (XP) scoring mode in Glide of Schrödinger 9.0 software package.3 Detailed Glide docking procedures can be seen in the previous study [7]. The binding pose of Zharp1-211 and important interaction patterns between Zharp1-211 and RIPK1 were illustrated and discussed in Figure S6D.

qPCR

Total RNA was extracted from organoids or cells using a MicroElute total RNA kit (R6831, Omega). RNA was reversely transcribed into cDNA using cDNA Synthesis Supermix (E043, Novoprotein) according to the manufacturer's protocol. The gene expression was detected by q PCR using SYBR Green Master Mix (B21202, Bimake). The PCR reaction was performed on the Roche LightCycler 480 II system. Gene expression was normalized to *Gapdh*. Primers were used as follows: Mouse Ccl5: GCTGCTTTGCCTACCTCTCC (sense); TCGAGTGACAAACACGACTGC (antisense). Mouse Cxcl9: CCACTACAAATCCCTCAAAGAC (sense); TCTAGGCAGGTTTGATCTCC-3' (antisense). Mouse Cxcl10: CGTCATTTTCTGCCTCATCC (sense); GCAATGATCTCAACACGTGG (antisense). Mouse CIITA: TGCGTGTGATGGATGTCCAG (sense); CCAAAGGGGATAGTGGGTGTC (antisense). Mouse H2-DMB: ACCCCACAGGACTTCACATAC (sense); GGATACAGCACCCCAAATTCA (antisense). Mouse Ripk3: TTCCACATACTTTACCCTTCAGAG (sense); ATACTTGGCCGAACTTGAGG (antisense). Human Cxcl9: CCAGTAGTGAGAAAGGGTCGC (sense); AGGGCTTGGGGCAAATTGTT-3' (antisense). Human Cxcl10: GTGGCATTCAAGGAGTACCTC (sense); TGATGGCCTTCGATTCTGGAT (antisense). Gapdh: CAAGAAGGTGGTGAAGCAGGC (sense); CATACCAGGAAATGAGCTTGAC (antisense).

Flow cytometry

Anti-CD16/32 (2.4G2) was used to block non-specific staining. For surface staining, cell suspensions were incubated 2 μg per ml of following fluorochrome conjugated antibodies at 4 °C for 20min: CD45 (30-F11), CD3 (17A2), CXCR3 (CXCR3-173), CCR5 (HM-CCR5), EpCAM (G8.8), MHC class II (M5/114.15.2). 7-AAD (559925, BD) was added before cell examination. For intracytoplasmic staining, cell suspensions were incubated with fixable live/dead cell dye (65-0863-14, eBiosciense), blocked with Anti-CD16/32 and stained for surface markers. Cells were then fixed and permeabilized with the BD Fix/Perm kit (554714, BD) according to the manufacturer's instructions and stained with anti-IFN-γ (XMG1.2) for 30 min at room temperature. All samples were examined using Attune NxT Flow Cytometer (Thermo Fisher Scientific) and analyzed with FlowJo software (BD).

RNA sequencing and analysis

RNA samples were prepared from fresh intestines from mice experiencing GVHD or human biopsies. Total RNA was made to strain-specific cDNA library for sequencing with NEB Next Ultra II Directional RNA Library Prep Kit (E7760S, NEB) and sequenced on NovaSeq 6000 (Illumina). The reads were mapped to Ensembl hg19 (human) or GRCm38.p6 (mice) reference genomes and normalized using 'RNA-Seq Analysis' program of CLC genomic workbench 12.0 (Qiagen). Fold changes and p-values of genes between groups (triplication for each group) were calculated by 'Differential Expression in Two Groups' program in CLC genomic workbench 12.0. The top most significantly differentially expressed genes (fold change >=2, with an FDR p-value < 0.05 between two groups) were considered for subsequent functional enrichment using Geneset Enrichment Analysis. We preformed the gene set enrichment analysis (GSEA) on the hallmark gene sets using GSEAPreranked test[8]. The results were visualized in volcano maps using the drawing packages "ggplot2" and "ggrepel". For each gene across all samples, the relative FPKM values were calculated, and the scaled FPKM values were used to generate heatmaps.

Quantification and statistical analysis

Graphs and statistical analyses were performed using Prism software version 9.02

(GraphPad Software, La Jolla California, USA, https://www.graphpad.com). Data shown in figures are mean ± SD, except for weight curves, histology scores and chemokines concentration which are mean ± SEM.. Survival rates across different groups were compared using the log-rank test; 2-tailed Student's t test was used for 2-group comparisons, and 1-way ANOVA with Tukey's multiple-comparison test was used for multiple comparisons with *p < 0.05; **p < 0.01; ***p < 0.001; ****p < 0.0001; n.s., not significant. All values are calculated from at least three independent biological replicates, unless otherwise stated. RNA-Seq data were analyzed by 'Differential Expression in Two Groups' program in CLC genomic workbench (Qiagen).

Plasma Protein Binding (PPB) assay

The PPB assay of **Zharp1-211** (HCl salt) in mouse/rat/human plasma was evaluated using equilibrium dialysis at Chempartner. During the experiment, **Zharp1-211** was spiked into plasma to achieve the concentration of 1 μM. The compound spiked plasma was kept in the donor side, and blank PBS buffer was kept in the receiver side. The dialysis block was covered with a plastic lid and incubated in a shaker (60 rpm) for 5 hours at 37 ℃. The donor and receiver sides were collected after the incubation. PPB rate was calculated using the following equation. The result was shown in **Supplemental Figure 6.**

$$\text{PPB (\%)} = \frac{100 \times (\text{donor}_{5h}\text{-receiver}_{5h})}{\text{donor}_{5h}}$$

Evaluation of CYP inhibitory potency

Inhibitory potency of **Zharp1-211** (HCl salt) against human P450 enzymes was investigated in human liver microsomes. The five major CYP isoforms and their respective probe substrates were as follows: CYP3A4 (midazolam, 5 μM), CYP2D6 (bufuralol, 10 μM), CYP1A2 (phenacitine, 30 μM), CYP2C9 (diclofenac, 10 μM), and CYP2C19 (S-mephenytoin, 35 μM). All probe substrates were used at concentrations near or below their K_ms (Michaelis constant). Duplicate incubations were conducted in

the 200 μL incubation mixtures at 37 ℃. The mixture contained HLM from corning, phosphate buffer (100 mM, pH 7.4), NADPH (1 mM), tested compounds (10 μM), and individual CYP probe substrate. The mixtures were pre-incubated for 5 min to allow inhibitor/enzyme interactions before the initiation of the reaction with NADPH. Incubation the assay plate at 37 °C. 5 min for 3A4, 10 min for 1A2, 2C9 and 2D6, and 45 min for 2C19, the reactions were terminated by the addition of 120 μM of cold acetonitrile containing an appropriate internal standard. Samples were then centrifuged and injected into the LCMS/MS apparatus to quantify the concentrations of specific metabolites formed by individual CYP enzymes. The result was shown in **Supplemental Figure 6.**

hERG assay

Zharp1-211 (HCl salt) was evaluated for block of the hERG potassium channel at Chempartner using CHO cells stably expressing the hERG gene and the QPatch platform (Sophion, Ballerup, Denmark). K tail currents were measured at -50 mV following a 500 ms depolarization to +20 mV from a holding voltage of -80 mV. The external solution contained 4 mM K^+, 1 mM Mg^{2+}, and 2 mM Ca^{2+}. Compound's effect was quantified 4 min after application to the cells. Pulses were elicited every 20 s. The result was shown in **Supplemental Figure 6.**

PK study *in vivo*

Single dose pharmacokinetic parameters were determined at Medicilon using male ICR mouses (24 mouses per group, 2 groups) and male SD rats (3 rats per group, 2 groups). Groups were dosed i.v. (2 mg/kg) or p.o. (10 mg/kg) and blood samples taken via submandibular or saphenous vein at the following time points post dosing: 0.083 (i.v. only), 0.25, 0.5, 1, 2, 4, 6 (p.o. only), 8 and 24 h. An aliquot of 50 μL of blood plasma was protein precipitated with 250 μL internal standard solution (200 ng/mL tolbutamide in MeOH), the mixture was vortex-mixed for 1 min and centrifuged at 14,000 rpm for 5 min. The concentration of **Zharp1-211** (HCl salt) in the plasma samples was determined using LC-MS/MS with the peak areas compared to a calibration curve determined using 5-5000 ng/mL **Zharp1-211** in male ICR mouse or SD rat plasma. The results were shown in **Supplemental Figure 7.**

Detailed synthetic procedure for Zharp1-211 and its analogs

General reaction progress was monitored by analytical thin layer chromatography performed on silica gel HSGF254 pre-coated plates. Organic solutions were dried over anhydrous Na_2SO_4, and the solvents were removed under reduced pressure. Final compounds were purified with silica gel 100-200 mesh for column chromatography. ^1H NMR and ^{13}C NMR were obtained on 400 MHz (Varian) or 600 MHz (Varian) spectrometers. Chemical shifts were given in ppm using tetramethylsilane as internal standard. Data for ^1H NMR are reported as follows: chemical shift, multiplicity (s = singlet, d = doublet, t = triplet, q = quartet, m = multiplet, br = broad), coupling constants and integration. Mass spectra were obtained using an Agilent 1100 LC/MSD Trap SL version Mass Spectrometer. HRMS analysis was recorded on an Agilent 6540 UHD Accurate-Mass QTOF LC/MS. HPLC method: Waters Acquity UPLC, BEH C18 2.1 mm × 50 mm, 1.7 μm particles. Mobile phase A: 5 mM aqueous formic acid. Mobile phase B: MeOH. Temperature: 24 °C. Gradient: 5−40% B over 1 min, 40-70% B over 1 min, 70-95% B over 4 min, then a 1 min hold at 95% B. Flow: 1.2 mL/min. Detection: UV at 254 nm. Melting points were determined by a SMP10 melting point apparatus.

- **Zharp1-211-2**: ***N*-(5-Bromopyridin-2-yl)-4-methylbenzenesulfonamide**

A mixture of **Zharp1-211-1** (20.0 g, 116 mmol) and TsCl (24.2 g, 127 mmol) in 80 mL pyridine was stirred at 90 °C overnight. The reaction mixture was cooled to room temperature and concentrated. Water (200 mL) was poured into the residue. The resulting precipitate was filtered, then washed with water (20 mL) to give the desired product (35.5 g, 93 %) as a white solid. ^1H NMR (400 MHz, DMSO-d_6) δ 11.24 (br s, 1H), 8.27 (s, 1H), 7.89 (d, J = 8.0 Hz, 1H), 7.78 (d, J = 8.0 Hz, 2H), 7.37 (d, J = 8.0 Hz, 2H), 7.03 (d, J = 8.8 Hz, 1H), 2.35 (s, 3H). MS (ESI/APCI) m/z 326.7 $[M+H]^+$.

- **Zharp1-211-3**: **(*Z*)-2-(5-Bromo-2-(tosylimino)pyridin-1(2H)-yl)acetamide**

A mixture of **Zharp1-211-2** (32.7 g, 100 mmol), DIPEA (16.7 g, 129 mmol) and 2-iodoacetamide (23.9 g, 129 mmol) in 80 mL DMF was stirred at room temperature overnight. The reaction mixture was poured into ice water (1000 mL). The resulting precipitate was filtered to give the crude product as a white solid. The crude product was suspended in dichloromethane (200 mL) and stirred for 2 h, then filtered to give the desired product (35.0 g, 91%) as a white solid. ^1H NMR (400 MHz, DMSO-d_6) δ

8.38 (s, 1H), 7.88 (d, J = 9.6 Hz, 1H), 7.79 (s, 1H), 7.65 (d, J = 7.2 Hz, 2H), 7.41 (br s, 1H), 7.30-7.26 (m, 3H), 4.78 (s, 2H), 2.34 (s, 3H). ^{13}C NMR (150 MHz, DMSO-d_6) δ 167.5, 154.5, 144.1, 142.5, 141.9, 141.0, 129.6, 126.3, 117.7, 102.4, 54.8, 21.3. MS (ESI/APCI) m/z 383.7 $[M+H]^+$.

- **Zharp1-211-4**: ***N*-(6-Bromoimidazo[1,2-a]pyridin-2-yl)-2,2,2-trifluoroacetamide**

To a stirred solution of **Zharp1-211-3** (18.0 g, 46.0 mmol) in 200 mL dichloromethane at 0 °C was added TFAA (48.3 g, 230 mmol) dropwise. The mixture was stirred at 0 °C for 5 h. The mixture was neutralized using saturated $NaHCO_3$ solution to pH = 7. The resulting precipitate was filtered to give the crude product as a white solid. The crude product was suspended in dichloromethane (150 mL) and stirred for 2 h, then filtered to give the desired product (11.1 g, 78%) as a white solid. ^{1}H NMR (400 MHz, DMSO-d_6) δ 12.54 (s, 1H), 8.96 (s, 1H), 8.24 (s, 1H), 7.51 (d, J = 9.6 Hz, 1H), 7.41 (d, J = 8.8 Hz, 1H). MS (ESI/APCI) m/z 307.6 $[M+H]^+$.

- **Zharp1-211-5**: ***N*-(6-Bromoimidazo[1,2-a]pyridin-2-yl)cyclopropanecarboxamide**

To a solution of **Zharp1-211-4** (11.0 g, 36 mmol) in MeOH (100 mL) was added 1N NaOH aqueous solution (43 mL, 43 mmol). The mixture was stirred at 80 °C overnight. The mixture was cooled to room temperature and concentrated. The residue was dissolved in dichloromethane (150 mL) and washed with sat. aq. NaCl (100 mL*2). The organic phase was dried over Na_2SO_4, filtered and concentrated to give a yellow solid (8.0 g, crude). To a solution of the yellow solid in dichloromethane (150 mL) was added dropwise TEA (4.0 g, 40 mmol) and the cyclopropanecarbonyl chloride (4.2 g, 40 mmol) in dichloromethane solution (50 mL) successively at 0 °C, then stirred for 3 h at the same temperature. The reaction solution was quenched with sat. aq. K_2CO_3 (50 mL). The mixture was concentrated to 1/4 of the initial volume, then filtered to give the desired product (7.8 g, 78%) as a white solid. MP: 247-249 °C. ^{1}H NMR (400 MHz, DMSO-d_6) δ 11.03 (s, 1H), 8.87 (s, 1H), 8.06 (s, 1H), 7.40 (d, J = 9.2 Hz, 1H), 7.30 (d, J = 9.6 Hz, 1H), 1.94-1.92 (m, 1H), 0.81-0.79 (m, 4H). ^{13}C NMR (150 MHz, DMSO-d_6) δ 171.5, 142.9, 139.8, 127.4, 126.9, 116.6, 105.4, 101.5, 14.1, 7.8. MS (ESI/APCI) m/z 279.7 $[M+H]^+$.

- **Zharp1-211-7**: **Tetrahydro-2H-pyran-4-yl carbonochloridate**

To a solution of BTC (11.5 g, 38 mmol) in dichloromethane (80 mL) was added pyridine (8.3 g, 8.5 mL,105 mmol) dropwise at 0 °C, then added **Zharp1-211-6** (10.2 g, 95 mmol) at the same temperature. The mixture solution was stirred at 0 °C for 2 h, then filtered. The filtrate was concentrated, then diluted with ethyl acetate (100 mL). The mixture was stirred at room temperature for 0.5 h, then filtered. The filtrate was concentrated to give the desired product (16.0 g, crude) as a colorless oil. ^{1}H NMR (400 MHz, $CDCl_3$) δ 5.10-4.93 (m, 1H), 3.94-3.91 (m, 2H), 3.55-3.50 (m, 2H), 2.11-2.00 (m, 2H), 1.89-1.80 (m, 2H).

- **Zharp1-211-9**: **Diethyl 2-(5-bromo-3-nitropyridin-2-yl)malonate**

To a suspension of NaH (60%, 1.2 g, 30 mmol) in THF (50 mL) was added dropwise diethyl malonate (4.8 g, 30 mmol) at 0 °C. The mixture was stirred at 0 °C for 0.5 h, then the solution of **Zharp1-211-8** (2.4 g, 10 mmol) in THF (10 mL) was added dropwise. The reaction was stirred at 0 °C for another 2 h. Sat. aq. NH_4Cl (20 mL) was added to quench the reaction. The mixture was diluted with ethyl acetate (100 mL) and washed with sat. aq. NaCl (30 mL × 3). The organic phase was dried over Na_2SO_4, filtered and concentrated. The residue was purified by silica gel column chromatography (petroleum ether/ethyl acetate = 10/1) to give the desired product (3.4 g, 94%) as a colorless oil. ^{1}H NMR (400 MHz, $CDCl_3$) δ 8.87 (s, 1H), 8.62 (s, 1H), 5.45 (s, 1H), 4.32-4.27 (m, 4H), 1.31-1.29 (m, 6H). MS (ESI/APCI) m/z 360.6 $[M+H]^+$.

- **Zharp1-211-10**: **Ethyl 2-(3-amino-5-bromopyridin-2-yl)acetate**

A mixture of **Zharp1-211-9** (36.0 g, 100 mmol), LiCl (21.0 g, 500 mmol) and water (10 mL) in DMSO (150 mL) was stirred at 110 °C overnight. After the mixture was cooled to room temperature, diluted with ethyl acetate (400 mL) and washed with sat. aq. NaCl (200 mL × 3). The organic phase was dried over Na_2SO_4, filtered and concentrated to give a black oil (about 30.0 g). Then the black oil was dissolved in EtOH/H_2O (200 mL/100 mL). To a solution of the black oil NH_4Cl (27.0 g, 500 mmol) was added, Fe powder (16.8 g, 300 mmol) was added slowly at 80 °C. The suspended solution was stirred at 80 °C for 3 h, then filtered. The filtrate was concentrated to remove EtOH, then the residue was diluted with ethyl acetate (500 mL) and washed with sat. aq. NaCl (100 mL × 3). The organic phase was dried over Na_2SO_4, filtered and concentrated. The residue was purified by silica gel column chromatography

(petroleum ether/ethyl acetate = 3/1) to give the desired product (10.5 g, 41%) as a white solid. ^{1}H NMR (400 MHz, DMSO-d_6) δ 7.75 (d, J = 1.2 Hz, 1H), 7.17 (d, J = 1.6 Hz, 1H), 5.50 (s, 2H), 4.10-4.07 (q, J = 7.2 Hz, 2H), 3.66 (s, 2H), 1.17 (t, J = 7.2 Hz, 3H). ^{13}C NMR (150 MHz, $CDCl_3$) δ 170.6, 142.8, 140.1, 138.9, 125.1, 119.7, 61.5, 41.2, 14.1. MS (ESI/APCI) m/z 258.7 $[M+H]^+$.

- **Zharp1-211-11**: **Ethyl 2-(5-bromo-3-((((tetrahydro-2H-pyran-4-yl)oxy)carbonyl)amino)pyridin-2-yl)acetate**

To a solution of **Zharp1-211-10** (1.3 g, 5.0 mmol) and pyridine (990 mg, 1.0 mL, 12.5 mmol) in THF (30 mL) was added the solution of **Zharp1-211-7** (1.1 g, 6.8 mmol) in THF (10 mL) at 0 °C. The reaction was stirred at 0 °C for 2 h, then quenched with sat. aq. $NaHCO_3$ (10 mL). The mixture was diluted with ethyl acetate (50 mL), and the mixture was washed with sat. aq. NaCl (20 mL × 3). The organic phase was dried over Na_2SO_4, filtered and concentrated. The residue was purified by silica gel column chromatography (petroleum ether/ethyl acetate = 3/1) to give the desired product (1.6 g, 83%) as a colorless oil. ^{1}H NMR (400 MHz, $CDCl_3$) δ 8.43 (s, 1H), 8.33 (s, 1H), 8.28 (s, 1H), 4.96 (br s, 1H), 4.24-4.18 (q, J = 6.8 Hz, 2H), 3.98-3.95 (m, 2H), 3.87 (s, 2H), 3.58-3.53 (m, 2H), 2.02-2.00 (m, 2H), 1.78-1.75 (m, 2H), 1.30 (t, J = 7.2 Hz, 3H). MS (ESI/APCI) m/z 386.7 $[M+H]^+$.

- **Zharp1-211-12**: **Tetrahydro-2H-pyran-4-yl (5-bromo-2-(2-hydroxyethyl)pyridin-3-yl)carbamate**

To a solution of **Zharp1-211-11** (10.4 g, 27 mmol) in EtOH (150 mL) was added $NaBH_4$ (4.1 g, 108 mmol) slowly at 0 °C. The reaction was stirred at room temperature overnight, then the EtOH was removed. The residue was diluted with ethyl acetate (200 mL) and washed with sat. aq. NaCl (100 mL × 3). The organic phase was dried over Na_2SO_4, filtered and concentrated to give the desired product (9.8 g, crude) as a yellow oil. ^{1}H NMR (400 MHz, $CDCl_3$) δ 8.40 (s, 1H), 8.31 (s, 1H), 7.81 (s, 1H), 4.97-4.92 (m, 1H), 4.08 (s, 2H), 3.97-3.94 (m, 2H), 3.63-3.49 (m, 2H), 2.97 (t, J = 5.2 Hz, 2H), 2.05-1.95 (m, 2H), 1.80-1.70 (m, 2H). MS (ESI/APCI) m/z 344.7 $[M+H]^+$.

- **Zharp1-211-13**: **Tetrahydro-2H-pyran-4-yl6-bromo-2,3-dihydro-1H-pyrrolo[3,2-b]pyridine-1-carboxylate**

To a solution of **Zharp1-211-12** (9.8 g, about 27 mmol) and TEA (3.0 g, 29.7 mmol) in dichloromethane (150 mL) was added the solution of mesyl chloride (3.4 g, 29.7 mmol) in dichloromethane (30 mL) dropwise at 0 °C. The reaction was stirred at 0 °C for 2 h, then quenched with sat. aq. $NaHCO_3$ (50 mL). The mixture was diluted with dichloromethane (200 mL) and washed with sat. aq. NaCl (100 mL × 3). The organic phase was dried over Na_2SO_4, filtered and concentrated to give a brown oil. A mixture of the brown oil and Cs_2CO_3 (13.2 g, 40.5 mmol) in 1,4-dioxane (150 mL) was stirred at 110 °C overnight. The mixture was cooled to room temperature, then filtered. The filtrate was concentrated and purified by silica gel column chromatography (petroleum ether/ethyl acetate = 1/1) to give the desired product (4.7 g, two steps yield: 52%) as a white solid. MP: 117-119 °C. ^{1}H NMR (400 MHz, DMSO-*d*$_6$) δ 8.17 (s, 1H), 8.08-7.54 (m, 1H), 5.05-4.83 (m, 1H), 4.13-3.95 (m, 2H), 3.89-3.73 (m, 2H), 3.52 (t, *J* = 7.6 Hz, 2H), 3.14 (t, *J* = 8.0 Hz, 2H), 2.06-1.83 (m, 2H), 1.76-1.51 (m, 2H). ^{13}C NMR (150 MHz, $CDCl_3$) δ 152.3, 151.9, 143.8, 138.3, 123.7, 119.1, 70.8, 65.2, 46.4, 32.0, 29.1. MS (ESI/APCI) m/z 326.7 $[M+H]^+$.

- **Zharp1-211**: **Tetrahydro-2H-pyran-4-yl 6-(2-(cyclopropanecarboxamido)imidazo[1,2-a]pyridin-6-yl)-2,3-dihydro-1H-pyrrolo[3,2-b]pyridine-1-carboxylate**

A mixture of **Zharp1-211-13** (5.2 g, 16.1 mmol), bis(pinacolato)diboron (5.0 g, 19.7 mmol), potassium acetate (4.0 g, 41 mmol) and Pd(dppf)Cl_2 (512 mg, 0.70 mmol) in 1,4-dioxane (100 mL) was stirred at 100 °C overnight under N_2 atmosphere. The reaction was cooled to room temperature. **Zharp1-211-5** (3.9 g, 14.0 mmol), K_2CO_3 (4.8 g, 35 mmol), water (10 mL) and Pd(dppf)Cl_2 (256 mg, 0.35 mmol) were added successively. The mixture was stirred at 100 °C for another 5 h under N_2 atmosphere. The mixture was cooled to room temperature, filtered and concentrated. The residue was purified by silica gel column chromatography (dichloromethane/methanol = 30/1) to give the desired product (2.8 g, 44%) as a white solid. ^{1}H NMR (400 MHz, DMSO-*d*$_6$) δ 11.01 (s, 1H), 8.92 (s, 1H), 8.38 (s, 1H), 8.12 (s, 2H), 7.53-7.46 (m, 2H), 4.96 (br s, 1H), 4.08 (s, 2H), 3.84-3.82 (m, 2H), 3.55-3.52 (m, 2H), 3.24-3.20 (m, 2H), 1.94 (s, 3H), 1.65 (br s, 2H), 0.82-0.80 (m, 4H). ^{13}C NMR (100 MHz, $CDCl_3$) δ 171.8, 153.0, 152.7, 142.7, 141.3, 140.8, 137.6, 131.7, 125.1, 123.8, 123.3, 119.2, 115.4, 101.6, 70.8, 65.2, 46.2, 32.0, 29.3, 14.9, 8.1. HRMS (ESI): calcd for $C_{24}H_{25}N_5O_4$ $[M+H]^+$448.1979, found 448.1979. Purity: 98.8%.

Caco-2 permeability assay

The Caco-2 permeability study of **Zharp1-211** (HCl salt) was performed at ChemPartner. Caco-2 cells were obtained from American Tissue Culture Collection (Rockville, MD). The cells were maintained in Modified Eagle's medium (MEM), containing 10% heat-inactivated fetal bovine serum, and 1% non-essential amino acids, in CO_2 at 37 °C. Cells were seeded on polycarbonate filter inserts (Millipore, CAT#PSHT 010 R5).

The cells were cultured for 21-28 days prior to the transport experiments. The transepithelial electric resistance and Lucifer Yellow permeability were checked before and after the assay. **Zharp1-211** was dissolved at 10 mM in 100% dimethyl sulfoxide (DMSO) and diluted for studies in Hanks Balanced Salt Solution (HBSS, Invitrogen, Cat# 14025-092) with 25 mM HEPES, pH 7.4. **Zharp1-211** was tested at 10 μM, and in both the apical-tobasolateral (A-B) and basolateral-to-apical (B-A) directions, and were conducted at 37 °C for 90 min. At the end of incubation, donor samples were diluted 10-fold by assay buffer, then 60 μL of receiver and diluted-donor samples were mixed with 60 μL of acetonitrile, and analyzed by LC-MS/MS. The concentrations of the compounds were quantified by standard curve. The result was shown in **Supplemental Figure 6.**

Reference

1 Liu, Y. *et al.* RIP1 kinase activity-dependent roles in embryonic development of Fadd-deficient mice. *Cell death and differentiation* 24, 1459-1469 (2017). https://doi.org:10.1038/cdd.2017.78

2 Leach, M. W., Bean, A. G., Mauze, S., Coffman, R. L. & Powrie, F. Inflammatory bowel disease in C.B-17 scid mice reconstituted with the CD45RBhigh subset of CD4+ T cells. *Am J Pathol* 148, 1503-1515 (1996).

3 Riesner, K., Kalupa, M., Shi, Y., Elezkurtaj, S. & Penack, O. A preclinical acute GVHD mouse model based on chemotherapy conditioning and MHC-matched transplantation. *Bone Marrow Transplant* 51, 410-417 (2016). https://doi.org:10.1038/bmt.2015.279

4 Yuan, H. *et al.* Histone methyltransferase SETD2 modulates alternative splicing to inhibit intestinal tumorigenesis. *The Journal of clinical investigation* 127, 3375-3391

(2017). https://doi.org:10.1172/JCI94292

5 Gokulan, K., Williams, K., Orr, S. & Khare, S. Human Intestinal Tissue Explant Exposure to Silver Nanoparticles Reveals Sex Dependent Alterations in Inflammatory Responses and Epithelial Cell Permeability. *Int J Mol Sci* 22 (2020). https://doi.org:10.3390/ijms22010009

6 Harris, P. A. *et al.* Discovery of Small Molecule RIP1 Kinase Inhibitors for the Treatment of Pathologies Associated with Necroptosis. *ACS medicinal chemistry letters* 4, 1238-1243 (2013). https://doi.org:10.1021/ml400382p

7 Hou, J. *et al.* Discovery of potent necroptosis inhibitors targeting RIPK1 kinase activity for the treatment of inflammatory disorder and cancer metastasis. *Cell death & disease* 10, 493 (2019). https://doi.org:10.1038/s41419-019-1735-6

8 Subramanian, A. *et al.* Gene set enrichment analysis: a knowledge-based approach for interpreting genome-wide expression profiles. *Proceedings of the National Academy of Sciences of the United States of America* 102, 15545-15550 (2005). https://doi.org:10.1073/pnas.0506580102